J Therm Anal Calorim (2016) 125:1095–1103
DOI 10.1007/s10973-016-5462-2

Effect of addition of BaO on sintering of glass–ceramic materials from SiO_2–Al_2O_2–Na_2O–K_2O–CaO/MgO system

Janusz Partyka[1] · Katarzyna Gasek[1] · Katarzyna Pasiut[1] · Marcin Gajek[1]

Received: 14 October 2015 / Accepted: 8 April 2016 / Published online: 25 April 2016

Abstract Glass–ceramic materials due to the various physical and chemical parameters have a more and more wide application in various areas of engineering. This paper presents a glass–ceramic material originating from the Al_2O_2–SiO_2–Na_2O–K_2O–CaO/MgO modified by the addition of barium oxide. For the oxide composition which the molar ratio of SiO_2/Al_2O_3 is constant and equal to 6.42, and containing 0.375 mol% of $Na_2O + K_2O$ and 0.625 mol% of MgO was introduced barium oxide in quantities: 4, 9 and 14 mass%. For research of the sintering process, the following thermal analysis techniques were used: differential scanning calorimetry, dilatometry measurement and hot-stage microscopy. Analysis of the observed thermal transitions, marked on the respective charts, allows for appropriate design of the sintering curves in order to obtain a material with a high degree of crystallisation. The results of thermal analysis were compared with the phase compositions determined by X-ray diffraction and images from electron scanning microscopy of polished samples of glass–crystalline materials. Phenomena related to the influence of addition of barium oxide and heating treatment are analytically discussed.

Keywords Glass–ceramic · Sintering · Crystallisation · Crystalline · Phase composition

✉ Katarzyna Gasek
gasek@agh.edu.pl

Janusz Partyka
partyka@agh.edu.pl

[1] Department of Ceramics and Refractory Materials, Faculty of Material Science and Ceramics, AGH University of Science and Technology, al. A. Mickiewicza 30, 30-059 Kraków, Poland

Introduction

Glass–ceramic materials are produced through controlled crystallisation of a completely or partially melted raw material batch in a manner that allows for obtaining a fine-grained crystalline structure in the crystalline phase matrix. The material obtained in this way should be characterised by lack of porosity and an appropriately selected degree of re-crystallisation [1–4]. Designing the input oxide composition and the selection of the firing curve determine the type and quantity of the resulting crystalline phase and the chemical composition of the vitreous phase bonding crystallite grains [1, 2, 4]. The final phase composition determines the performance of the material obtained.

The proposed multi-component oxide system, given as SiO_2–Al_2O_3–Na_2O–K_2O–CaO–MgO with an additive of BaO, is not commonly used for the production of technical glass–crystalline materials. Such compositions are more often used for the production of crystalline or glass–crystalline glazes. The most important components in the system being discussed include silicone oxides, which form the basic structural network and amphoteric aluminium oxide, which are built into the silico-oxide network by isomorphous substitutions of Al^{3+} ions instead of Si^{4+} [3, 4]. The SiO_2/Al_2O_3 ratio has the main influence on characteristic temperatures of the glass–crystalline materials, their crystallisation tendencies and thus the scope of their application [3–5, 8, 9]. Modifications of the characteristic temperatures can be obtained by introducing alkaline metal oxides, Na_2O and K_2O (low- and medium-temperature fluxing agents), or alkaline earth oxides CaO, MgO, BaO, etc. (medium- and high-temperature fluxing agents) [1, 2, 4, 6, 7].

Barium oxide, as the only fluxing agent in the group of alkaline earth oxides, is active even in a small amount, but only at temperatures above 1250 °C. However, in the

presence of alkaline metal oxides, BaO begins to co-form the liquid phase at a considerably lower temperature than 1000 °C, as in the SiO_2–BaO–K_2O system at a temperature of 907 °C [6, 7, 9, 11, 12] and in the SiO_2–BaO–Na_2O system at a temperature of 785 °C [11, 12]. The BaO additive effectively improves mechanical parameters and chemical resistance [1–3]. Sources of barium oxide include BaO-containing frits, barium sulphate ($BaSO_4$) and barium carbonate ($BaCO_3$). Barium sulphate, due to sulphur dioxide emissions during thermal processing, is used relatively rarely. Barium carbonate is also applied as a raw material to a limited extent, mostly due to its harmfulness to humans. Both raw materials can also pose problems related to the quality of surface in low-melting materials or materials with a low content of alkaline metal oxides. During thermal processing in an oxidising atmosphere, they decompose in the liquid vitreous phase rich in alkaline oxides (Na_2O, K_2O or Li_2O) and produce a large number of gaseous products, which cause surface defects, such as holes, pinholes or blisters situated near the surface. However, if released, BaO quickly reacts with the oxygen–aluminium–silicon lattice of the vitreous phase; barium oxide reacts with other oxides causing crystallisation of new phases under favourable conditions [10, 11].

Research methodology

The research focused on two glass–crystalline materials with the composition selected from among the multi-component system of SiO_2–Al_2O_3–Na_2O–K_2O–CaO/MgO, into which BaO was introduced in the mass amounts of 4, 9 and 14 %, over 100 % of the base material. Molar base compositions of the materials, without the additive of barium oxide, are presented in Table 1. Naturally enriched natural raw materials were used in the study: Sibelco Norfolat K600 and Na600 feldspars, Sobótka MK40 silica powder, Ottavi wollastonite, Luzenac talc and Surmin KOC kaolin. The compositions of the raw materials were calculated using the SEGER software developed in the course of the project. Sample preparation consisted in grinding individual compositions in a planetary ball mill for 40 min, resulting in residues of 0.8 ± 0.05 % by mass on the 56-μm sieve. Once dried to obtain a constant mass at 150 °C, some powder was burnt in a porcelain crucible at 1230 °C. The raw powder was subject to thermal processing; in this case, the characteristic temperatures were measured and differential scanning calorimetry (DSC) was performed [9, 12, 13]. Using the thermally processed material, samples were cut out in the form of cuboids with dimensions of 4 × 4 × 10 mm for the purpose of dilatometric tests and the observation on an electron scanning microscope (SEM) with an EDS attachment. The remaining part underwent size reduction to below 56 μm, which was used for determination of the XRF oxide composition and XRD phase composition. For examination of the characteristic temperatures and thermal transformation, the following equipment was used:

Table 1 Oxide compositions of PORC 01-4 Ca/Mg base glass–ceramic materials

Description of glass-ceramic materials	SiO_2	Al_2O_3	CaO	MgO	$Na_2O + K_2O$
I PORC 01-4 Ca	70.45	10.75	11.69	0.36	6.75
I PORC 01-4 Mg	70.89	11.04	0.42	10.87	6.78

- HSM Misura 3 hot-stage temperature microscope, each measurement was carried out up to determine the melting temperature, increasing the temperature at a constant rate of 10° min^{-1};
- Netzsch DL 402C mechanical dilatometer, heating the samples at a constant rate of 10° min^{-1} to a temperature above the softening temperature;
- Netzsch STA 449 F3 Jupiter thermal analyser to test thermal transformation during thermal processing, heating the samples at a constant rate of 10° min^{-1} to a maximum temperature 1230 °C.

To determine other parameters, the following devices were applied:

- Spectrometer WDXRF Axios mAX with the RH lamp with a power 4 kW, analyser, to determine chemical composition;
- PANalytical X-ray diffractometer (X'Pert Pro), with scanning range was 5°–90° (2θ) at scanning rate of 0.05° 2θ/2 s with a recording speed of 0.05° 2θ/2 s, to determine the phase composition;
- NOVA NANO SEM 200 electron microscope with an EDS X-ray chemical microanalyser supplied by EDAX to observe the surface of microsections of the glass–ceramic materials.

Results and discussion

The chemical composition was investigated to verify the theoretical assumptions on the molar compositions used for the conversion into raw material batches and comparison with the composition of materials after grinding and burning. The results presented in Table 1, mostly the SiO_2/Al_2O_3 molar ratio and the CaO and MgO molar percentages, proved to be consistent with the assumptions. The almost identical additive of alkaline metal oxides is also essential. It proves that the presence of barium oxide is the only variable in both groups of the materials.

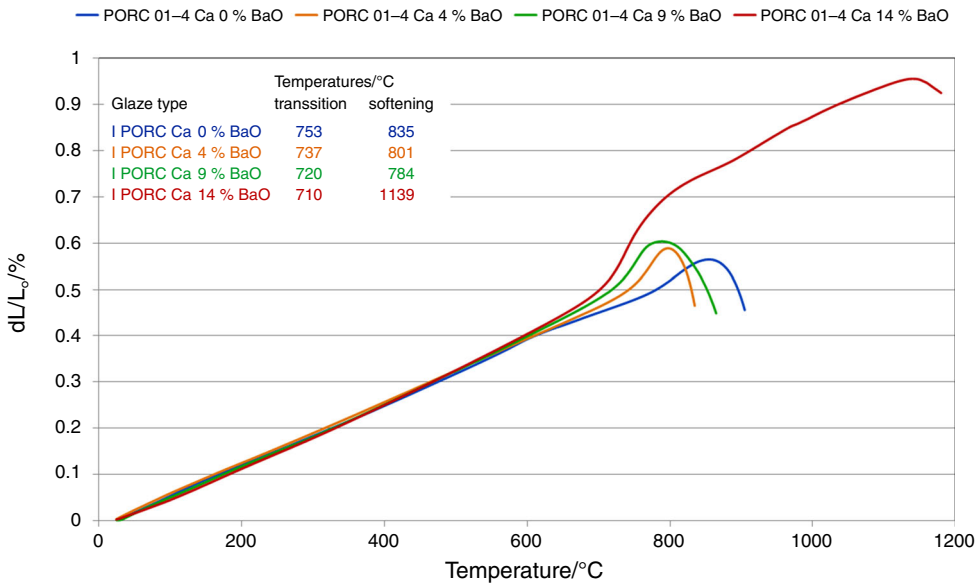

Fig. 1 Dilatometric curves of glass–ceramic glaze PORC 01-4 Ca + BaO with values of characteristic temperatures

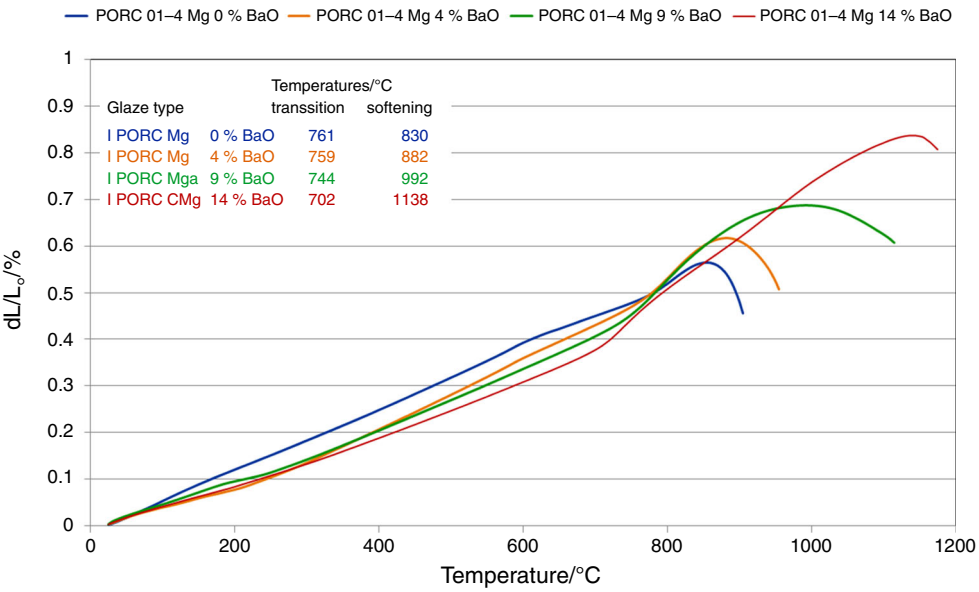

Fig. 2 Dilatometric curves of glass–ceramic glaze PORC 01-4 Mg + BaO with values of characteristic temperatures

The next step was aimed at investigating the influence of the barium oxide additive on the characteristic temperatures of the glass and crystalline materials in question. The tests were performed using the input material after grinding and drying. The measurement was taken until the total melt away of pastille was obtained (the height of the sample must be lower than one-third of the length of the base). The results of the measurements are presented in Table 2. The dilatometric characteristic temperatures, transition and softening, were conducted using the mechanical dilatometer Netzsch 402C. The samples, cuboid with dimensions of 10 × 5 × 5 mm, were cut from the glazes fired at a temperature of 1230 °C. The results dilatometric curves as a function of the temperature and values of the characteristic temperatures results are shown in Figs. 1, 2 and in Table 2.

By the analysis of the results obtained, it must be stated in the first place that the influence of the BaO additive on the characteristic temperatures depends on the type of the base material. In calcium materials, which contain CaO from alkaline earth oxides, the BaO additive reduces the values of individual characteristic temperatures, compared to the input material. The reduction in all temperatures is proportional to the quantity of the barium oxide additive. Particularly, visible changes concern the transition temperature (reduction by 43 °C) and the melting temperature

Table 2 Characteristic temperatures of tested glass–ceramic composites

Description of characteristic temperatures	I PORC 01-4 Ca				I PORC 01-4 Mg			
	Addition of Bao/mass%							
	0 %	4 %	9 %	14 %	0 %	4 %	9 %	14 %
	Temperature/°C							
Transition DL*	753	737	720	710	761	759	744	702
Softening DL*	835	801	784	1139	830	882	992	1138
Sphere—HSM**	1252	1247	1245	1230	1290	1299	1307	1298
Half-sphere—HSM**	1285	1270	1266	1250	1315	1324	1327	1318
Melting—HSM**	1324	1305	1296	1279	1335	1346	1344	1334

* Dilatometric

** Hot-stage microscope

(reduction by 45 °C). In other cases, the differences are as follows: reduction by 22 °C for the sphere temperature and by 35 °C for the hemisphere temperature. The influence on the characteristic temperatures of barium oxide increases together with its quantity; the influence is more noticeable at high temperatures. Thus, it may be concluded that in total, the results are consistent with these data relating to the materials in the system of SiO_2–Al_2O_3–Na_2O–K_2O–CaO. A different behaviour of various BaO additives was identified in the other tested system of SiO_2–Al_2O_3–Na_2O–K_2O–MgO, wherein magnesium oxide (MgO) is the representative of alkaline earth oxides in the base material. For the transition temperature, the material behaves in a similar manner, as was the case of the previously discussed system with the CaO additive; that is successive proportional reduction in this temperature to the increase in the BaO additive can be observed. As for the temperatures defined as the sphere, hemisphere and melting, the behaviour of the material is completely different. The sphere and hemisphere temperatures increase slightly from 9 to 12 °C for the 4 mass% and the 9 mass% additives of BaO. For the 14 mass% additive of BaO, the temperatures are reduced to the base material temperature, without the additive of the oxide. These differences can be accounted for by various levels of refractoriness of calcium and magnesium oxides and a higher tendency for crystallisation in systems with magnesium oxide. Another deviation from the described phenomena is the influence of the barium oxide additive on the dilatometric softening temperature in both systems. With the 4 and 9 mass% additive of BaO, changes in this temperature can be described exactly as for the sphere and hemisphere temperatures for systems with calcium and magnesium oxides, while for the 14 mass% additive of BaO, a sharp increase in the dilatometric softening temperature (by approximately 300 °C) is observed in both systems. The authors have not found an explanation for this effect yet. The most likely explanation is the large increase in the amount of crystalline phases in glazes containing 14 % by mass, barium oxide, in both types of material in the presence of calcium oxide and magnesium oxide (Fig. 9a, b).

Based on measurements of the characteristic temperatures, a graphic relationship between viscosity and temperature was determined. The Vogel–Fulcher–Tammann (VFT) equation was used for the calculations [14].

$$Log\,\eta = A + B/(T - T_0)$$

where A, B and T_0 are constants. Graphically, the VFT equation is represented with a straight-line plot of logη versus $1/(T–T_0)$, where A is the y-intercept, B is the slope of the line and T_0 is the measure of deviation of the curve from the ideal straight line of nonassociated liquids. The melt viscosity can be estimated from dilatometric and HSM measurements based on three known reference points: $\eta = 10^{12}$ Pa s as the dilatometric T_g; $\eta = 10^{9,25}$ Pa s as the dilatometric T_s; and $\eta = 10^{3,55}$ Pa s at the HSM $T_{1/2}$, where a sample forms a half-sphere shape during HSM analysis [14]. The results are presented in Figs. 3 and 4.

The introduction of barium oxide into the SiO_2–Al_2O_3–Na_2O–K_2O–CaO system influences the viscosity of the aluminium–silicon–oxygen alloy only for the case of the 14 mass% additive of BaO (Fig. 3). It can be seen that the parabolic nature of viscosity changes and the viscosity abruptly decreases from approximately 1250 °C. According to the authors, this change is mostly influenced by an unexplained rise in the value of the dilatometric softening temperature (T_s). For other amounts of this oxide, i.e. 4 and 9 mass%, the viscosity changes slightly, compared to the base material.

The BaO additive in the SiO_2–Al_2O_3–Na_2O–K_2O–MgO system exerts a considerably greater influence on the viscosity in the function of temperature. It is clear that the increase in the barium oxide additive results in the divergence of the viscosity logarithmic curves between 900 °C

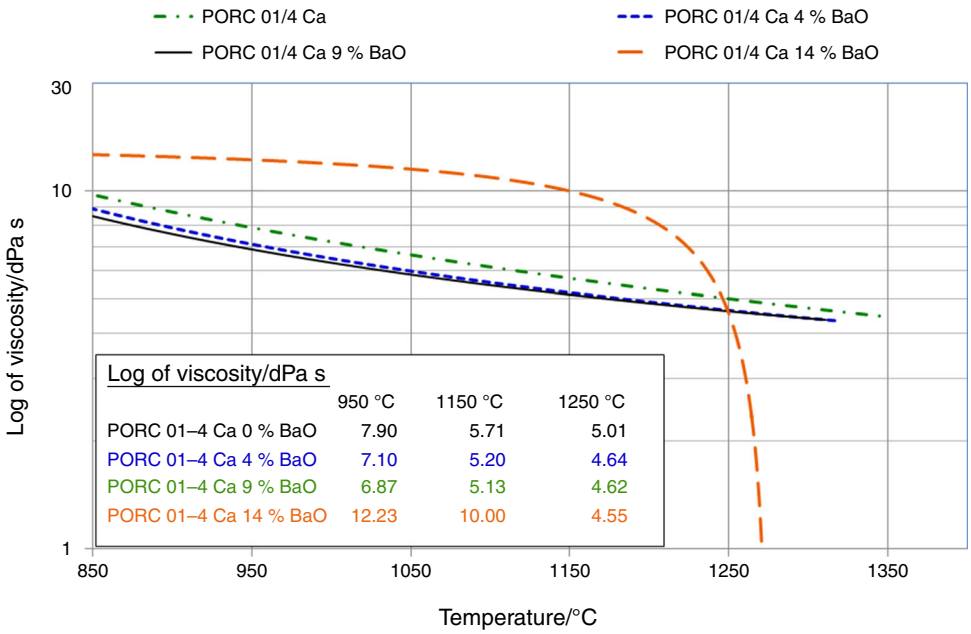

Fig. 3 Curves of log of the viscosity versus temperature for I PORC 01-4 Ca + BaO

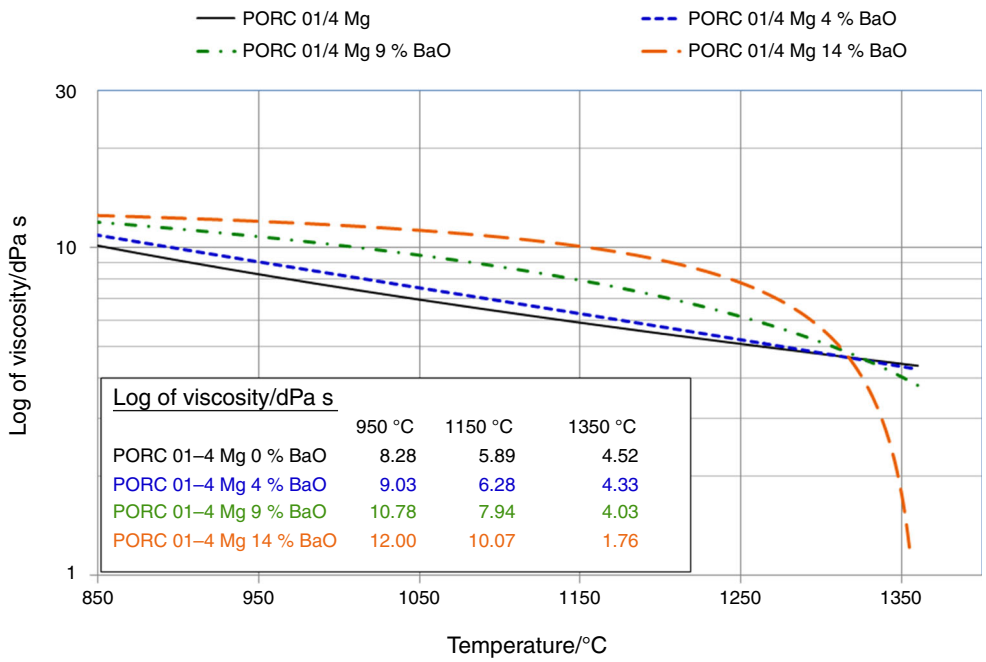

Fig. 4 Curves of log of the viscosity versus temperature for I PORC 01-4 Mg + BaO

and 1250 °C (Fig. 4); a higher BaO content results in a higher viscosity. Above 1250 °C, the viscosity curves begin to converge and achieve the same values at a temperature of approximately 1300 °C. An increase in the viscosity within the specified range of temperatures probably results from the occurrence of large amounts of crystalline phases in magnesium materials (Figs. 8, 9), as was the case of the changes in the characteristic temperatures. The logarithmic viscosity curve obtained for the 14 mass% additive shows a similar parabolic output to the analogous curve obtained for calcium materials. This similarity is caused by the same abrupt rise in the dilatometric softening temperatures as observed for the SiO_2–Al_2O_3–Na_2O–K_2O–CaO system.

In the next step, an attempt was made to explain the described phenomena by investigating the changes during thermal processing. For this purpose, thermal characteristics of the glass–crystalline materials were performed with

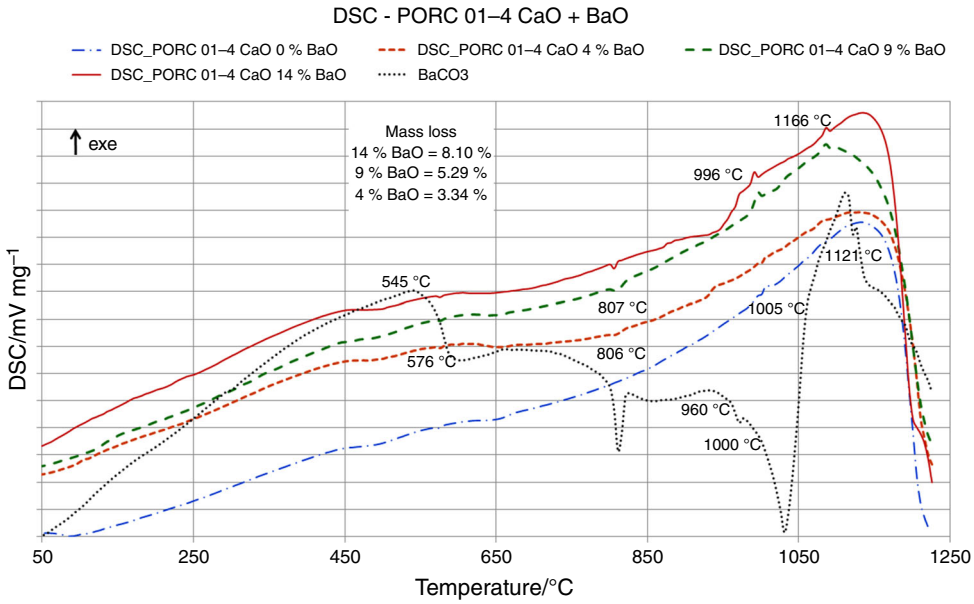

Fig. 5 Curve of DSC thermal transformations during thermal processing of the SiO_2–Al_2O_3–Na_2O–K_2O–CaO + BaO system

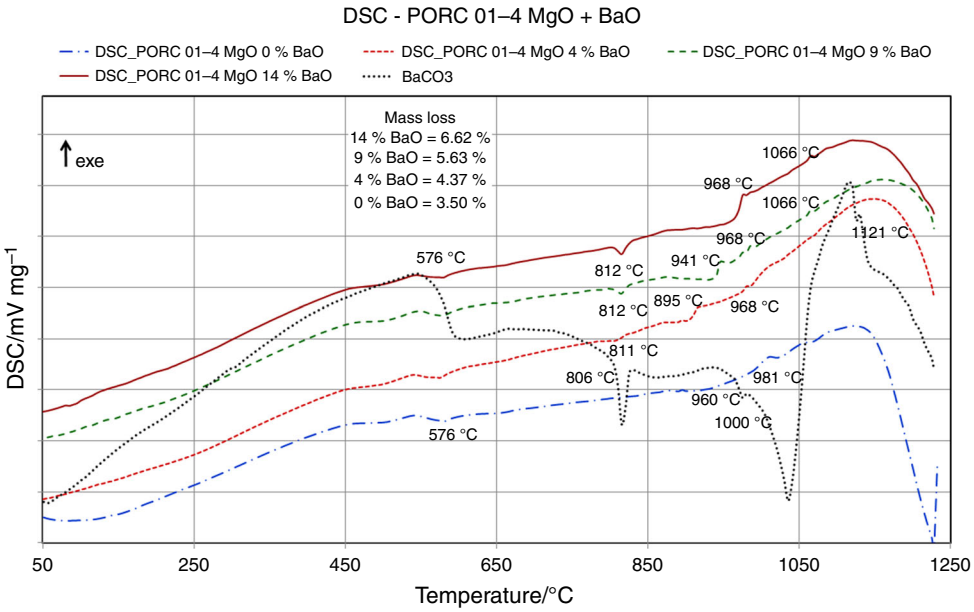

Fig. 6 Curve of DSC thermal transformations during thermal processing of the SiO_2–Al_2O_3–Na_2O–K_2O–MgO + BaO system

the DSC method using the Netzsch STA 449 F1 Jupiter apparatus in a synthetic air atmosphere with the heating rate of 10 °C min^{-1}. All measurements were taken while heating the materials to a temperature of 1230 °C at a rate of 10 °C min^{-1}. In order to facilitate the interpretation, the DSC curve obtained for barium carbonate, heated under the same conditions, was overlaid onto the graphs. The DSC sintering curves are presented in Figs. 5 and 6. The temperatures shown in the graphs are ONSET points, i.e. they occur at the beginning of the process.

In the graphs of the DSC lines relating to both tested systems of the glass–crystalline materials—SiO_2–Al_2O_3–Na_2O–K_2O–CaO and SiO_2–Al_2O_3–Na_2O–K_2O–MgO with the BaO additive—the effects seen in the barium carbonate distribution curve are reflected, i.e. mostly the endothermic effects starting in the carbonate at 806, 960 and 1000 °C (Figs. 5, 6). All other exothermic effects should correspond to crystallisation processes of new phases during the heating of the compositions with a various BaO content. For the SiO_2–Al_2O_3–Na_2O–K_2O–CaO system, these temperatures are equal to approximately 996 and 1066 °C for the 9 and 14 mass% additives (Fig. 5). These values should correspond to areas in which two crystalline phases present in these systems—sanidine and hyalophane—should be

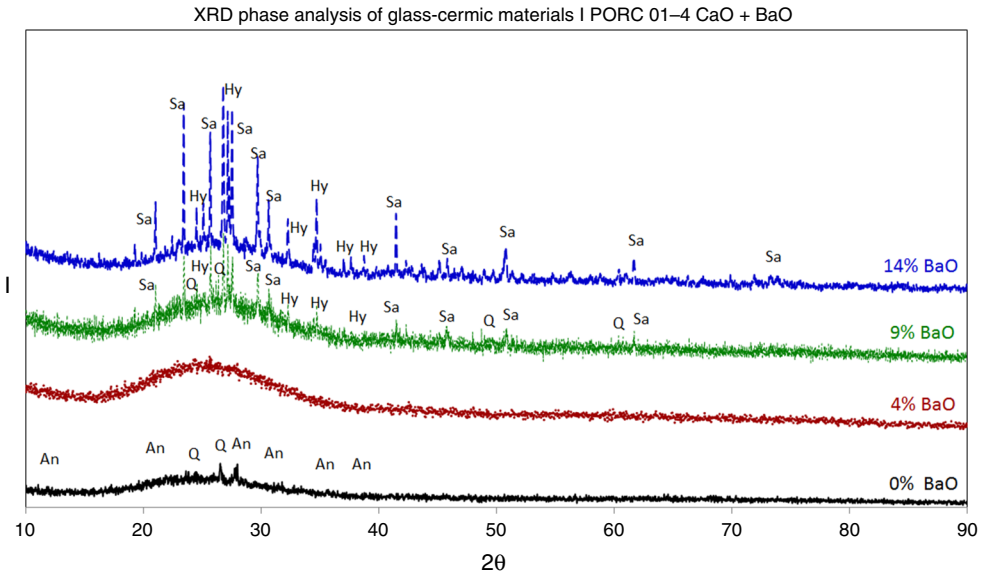

Fig. 7 XRD phase composition diagram for the glass–crystalline materials from the system composed of SiO_2–Al_2O_3–Na_2O–K_2O–CaO + BaO (Q—quartz, An—anorthite, Sa—sanidine, Hy—hyalophane)

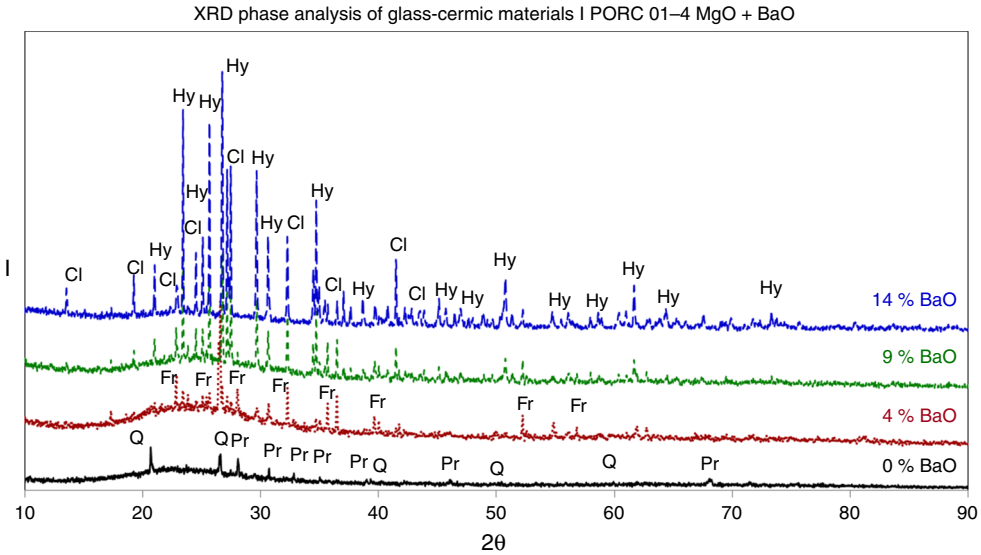

Fig. 8 XRD phase composition diagram for the glass–crystalline materials from the system composed of SiO_2–Al_2O_3–Na_2O–K_2O–MgO + BaO (Q—quartz, Pr—protoenstatite, Fr—forsterite, Hy—hyalophane, Cl—celsian)

formed (Figs. 7 and 8). The point, in which it is likely for anorthite to occur (Fig. 7) as regards the material without the BaO additive, should correspond to the peak on the DSC curve at approximately 1005 °C (Fig. 5).

The situation of the SiO_2–Al_2O_3–Na_2O–K_2O–MgO + BaO system is slightly different (Fig. 6). Admittedly, the effects which can be associated with the changes occurring while heating $BaCO_3$, i.e. endothermic effects at 806, 960 and 1000 °C, can be observed along the lines corresponding to the individual amounts of barium oxide. The effect observed at 981 °C should correspond to the occurrence of protoenstatite (Figs. 8 and 9). The remaining effects observable at 941, 968 and 1066 °C should show temperatures at which forsterite, hyalophane and celsian occur (Figs. 6, 8, 9).

Scanning electron microscopy images shows that the presence of BaO, in both types of materials, generally favours the crystallisation of crystalline phases, and additionally, it is in proportion to the increase in the content of barium oxide. In materials which contain MgO, the crystalline phase is definitely more. Both types of glazes (calcium and magnesium) exhibit different crystal habits due to the difference in the phase composition (Figs. 7, 8). The common crystal phase for both types of materials is only a barium alumino-silicate—hyalophane, and all other crystalline phases are different. The calcium glazes contain quartz, calcium alumino-silicate—anorthite—and potassium alumino-silicate—sanidine, and magnesium glazes contain magnesium silicate—forsterite, aluminium silicate—protoenstatite—and barium silicate—celsian.

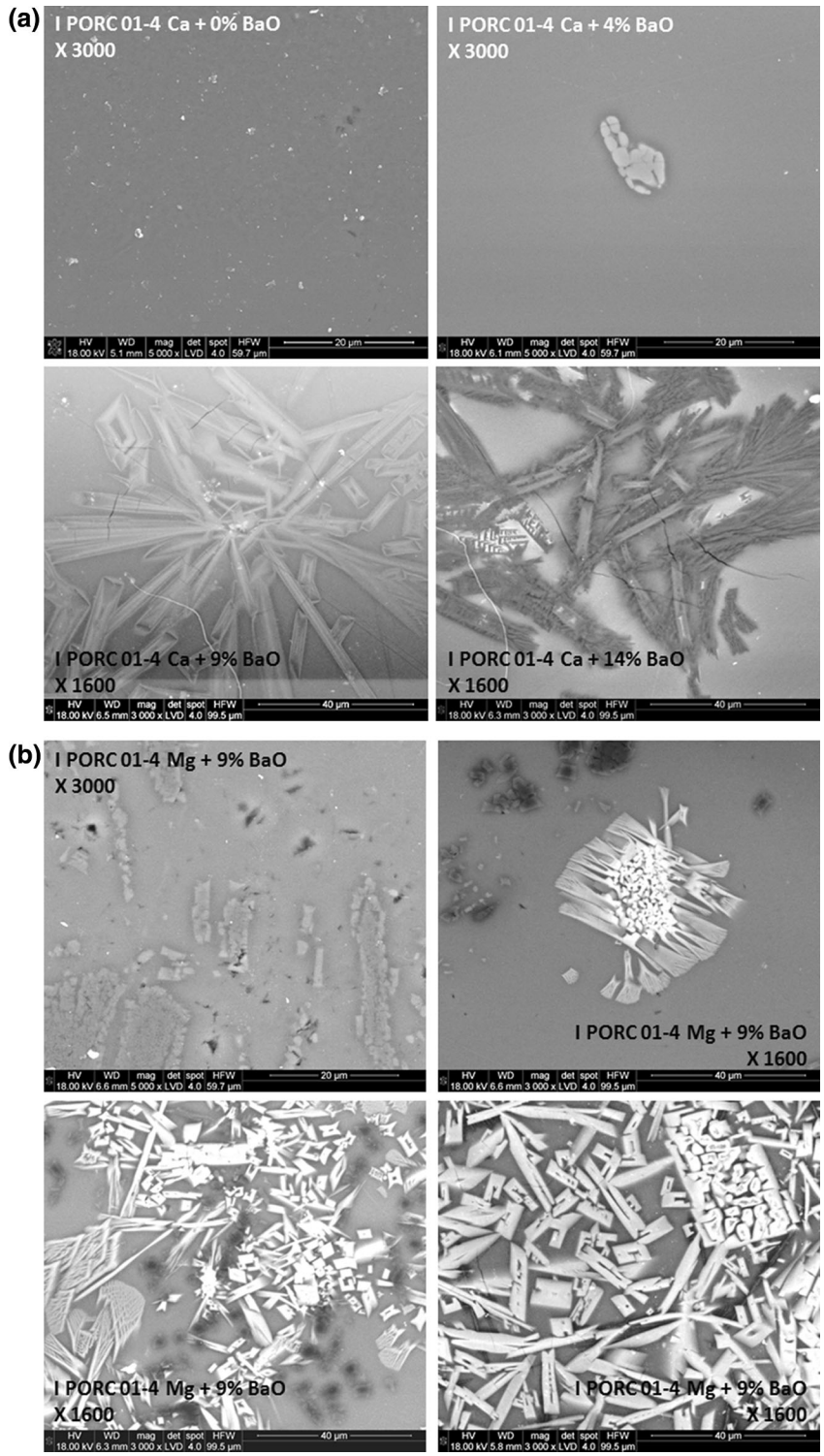

Fig. 9 SEM images of the glass–ceramic glazes samples from the systems composed of SiO_2–Al_2O_3–Na_2O–K_2O— **a** CaO/**b** MgO with the BaO additive

Conclusions

1. The additive of barium oxide has a considerable influence on both thermal properties and the phase composition of the obtained glass–crystalline materials.
2. The behaviour of barium oxide significantly depends on the composition of the base material and, as in the presented study, on the type of alkaline earth oxides, i.e. CaO and MgO.
3. In the thermal DSC analysis diagrams, it is possible to recognise the endothermic effects associated with the

decomposition of barium carbonate and exothermic effects resulting from the formation of new crystalline phases in the tested systems.

4. The tests of the phase composition using the XRD X-ray phase analysis and SEM-EDX scanning electron microscopy confirm the results of the thermal analyses, and as such, the type of crystalline phases and the texture of materials are defined.

Acknowledgements This research has been carried out thanks to financing under the framework of NCBiR (Polish National Research and Development Committee) programme Nos. N N508 477734 and PBS1/B5/17/2012.

References

1. Holand W, Beall GH. Glass ceramic technology. 2nd ed. London: Wiley; 2012. ISBN 978-0-470-48787-7.
2. Manfredini T, Pellacani GC, Rincon JM. Glass-ceramic materials. Fundamentals and applications. Modena: Mucchi Editore; 1997. ISBN-10: 887000287X.
3. Brow RK. Inorganic glasses and glass-ceramics chapter 6 in characterization of ceramics. Stoneham: Butterworth-Heinemann; 1993. p. 103–18.
4. Zachariasen WH. The atomic arrangement in glass. J Am Chem Soc. 1932;54:3841.
5. Gunawardane RP, Glasser FP. The System K_2O–BaO–SiO_2. J Am Ceram Soc. 1976;59(5-6):233–6.
6. Gunawardane RP, Glasser FP. Phase equilibria and crystallization of melts in the system Na_2O–BaO–SiO_2. J Am Ceram Soc. 1974;57(5):201–4.
7. ArgyleJ F, Hummel FA. System BaO–MgO–SiO_2; compatibility triangles. B = BaO; M = MgO; S = SiO_2. Glass Ind. 1965;46(12):710–8.
8. Chen J, Xiao X, Yang K, Wu H. Effect of Al_2O_3/SiO_2 Ratio on the viscosity and workability of high-alumina soda-lime-silicate glasses. J Chin Ceram Soc. 2012;40(7):1001–7.
9. Ahmed M, Earl A. Characterizing glaze melting behaviour via HSM Hot Stage Microscopy. Am Ceram Soc Bull. 2002;81(3):47–51.
10. Zhou W, Zhang L, Yang J. Preparation and properties of barium aluminosilicate glass-ceramics. J Mater Sci. 1997;32(18):4833–6.
11. Lambrinou L, Van der Bies O. Study of the devitrification behaviour of a barium magnesium aluminosilicate glass-ceramic. J Eur Ceram Soc. 2007;27:1805–9.
12. Szumera M. Charakterystyka wybranych metod termicznych. 2nd ed., LAB Laboratoria, Aparatura, Badania. 2013. 18(1), p. 24–33.
13. Qu LJ, Li B, Wang J, Gu YM. Application of DSC technique in study of glass ceramic. Adv Mater Res. 2010;105–106:743–5.
14. Paganelli M, Sighinolfi D. Understanding the behaviour of glazes with automatic heating microscope. Ceram Forum Int CFI/Ber DKG. 2008;85(5).